Journal of Fluorescence (2019) 29:9–14
https://doi.org/10.1007/s10895-018-2326-0

SHORT COMMUNICATION

Simple Way to Detect Trp to Tb^{3+} Resonance Energy Transfer in Calcium-Binding Peptides Using Excitation Spectrum

Petra Lišková[1] · Ivo Konopásek[1] · Radovan Fišer[1]

Received: 13 June 2018 / Accepted: 15 November 2018 / Published online: 23 November 2018

Abstract

The sensitized phosphorescence of Tb^{3+} is often used for the assessment of the ion binding to various chelating agents or natural Ca^{2+}-binding proteins. The detailed structure of the Tb^{3+} excitation spectrum gives a special advantage for analysis; any extra absorption peak can be easily detected which provides simple and direct evidence that resonance energy transfer occurs. By employing the Tb^{3+} phosphorescence, we characterized the Ca^{2+}-binding sites of two related peptides – self-processing module of the FrpC protein produced by bacterium *Neisseria meningitidis* and the shorter peptide derived from FrpC. Here we show that while the increase of direct Tb^{3+} excitation at 243 nm generally corresponds to Tb^{3+} association with various binding sites, the excitation enhancement in the 250–300 nm band signifies Tb^{3+}-binding in the close proximity of aromatic residues. We demonstrate that the presence of resonance energy transfer could be easily detected by inspecting Tb^{3+} excitation spectra. Additionally, we show that the high level of specificity of Tb^{3+} steady state detection on the spectral level could be reached at very low Tb^{3+} concentrations by taking advantage of its narrow phosphorescence emission maximum at 545 nm and subtracting the averaged autofluorescence intensities outside this peak, namely at 525 and 565 nm.

Keywords Terbium phosphorescence · Tryptophan · Protein fluorescence · Energy transfer · Excitation Spectrum · Calcium-binding site

Introduction

The characterization of binding of calcium ion into the protein molecule might still be challenging. Whereas direct spectroscopic determination of protein-bound calcium ions is almost impossible, trivalent luminescent ion of lanthanide terbium ($_{65}$Tb) may be used as a binding analogue of calcium [1–4]. Although terbium occurs in trivalent state, in contrast to divalent calcium, the similar ionic radii of both ions allow their substitutability (1.00 Å and 1.18 Å for Ca^{2+} and Tb^{3+}, respectively) [5, 6]. When bound to protein, Tb^{3+} increases its phosphorescence rate due to reduced quenching by water molecules and this sensitization is used routinely for Tb^{3+}-binding detection [3, 7]. The increase of intensity of Tb^{3+} phosphorescence bound to binding sites of single type proportionally corresponds to amount of ions and can be easily characterized e. g. by Hill function yielding the binding constants. Excitation and emission spectrum of terbium consists of series of peaks ranging from 240 nm to 700 nm that correspond to electron transitions between f → d orbitals [8–10]. As the electron engagement of terbium depends on electrostatic interactions, individual emission- and excitation peaks or bands differ greatly from bound state to non-bound state of the ion. Free terbium ion can be excited, for example, at a wavelength of ~240 nm and > 350 nm, bound terbium at 260–270 nm. In special case, bound Tb^{3+} can be excited via resonance energy transfer from fluorescent amino-acids (tryptophan or tyrosine) [4, 6, 11–13]. In this case, the Tb^{3+} absorption bands around 350 nm are involved (the transitions from the $^7F_6$ ground state to $^5L_9$, $^5D_2$, $^5G_5$ and $^5L_{10}$, $^5G_6$, $^5D_3$ levels) [14, 15] which overlap with emission spectrum of a nearby amino-acid. As the consequence such complex could be excited also at 270–290 nm where free Tb^{3+} practically does not absorb.

The purpose of this work was the comparison of Tb^{3+}-binding sites in the model Ca^{2+}-binding protein and in derived shorter peptide which still binds Tb^{3+}. As a small Ca^{2+}-binding molecule we used 29 amino-acids long "AFQ" synthetic peptide derived from so called SPM part (SPM, **S**elf **P**rocessing **M**odule) of the Ca^{2+}-binding protein FrpC produced by *Neisseria meningitidis* [16]. The SPM protein itself (177

✉ Radovan Fišer
radovan.fiser@natur.cuni.cz

[1] Department of Genetics and Microbiology, Faculty of Science, Charles University, Viničná 5, 128 43 Prague 2, Czech Republic

amino-acids) contains three predicted Ca^{2+}-binding sites (Fig. 2a) according to high sequence homology to EF-hands [16]. The binding of about five terbium or calcium ions to SPM was proven experimentally; at least one ion binds in a tight proximity of tryptophan residue Trp519 suggesting that this residue is important in Ca^{2+}-binding [17]. The AFQ peptide contains one of the expected calcium/terbium-binding motifs of SPM protein and a single tryptophan residue Trp519 (the number corresponds to the full-length FrpC protein). In particular, we asked whether this tryptophan residue is a part of the AFQ binding site or at least in the proximity to this site. The AFQ peptide molecule is so short that no other terbium ions are expected to specifically interact outside this predicted binding site. We demonstrated previously that the Tb^{3+}-binding sites on SPM protein correspond to Ca^{2+}-binding sites as could be deduced from the complete replacement of bound Tb^{3+} by the excess of added Ca^{2+} [17]. This allows the study of Ca^{2+}-binding sites on the SPM protein by means of increase of Tb^{3+} phosphorescence after direct excitation at 243 nm, as described earlier [17].

We found a simple and robust method for screening the properties of binding site (Fig. 1). We demonstrate here that Tb^{3+}-binding mode could be resolved easily by recording excitation spectra of Tb^{3+} at varying ion/peptide ratio.

Experimental

The production in *E. coli* BL21(λDE3) and isolation of the SPM protein was described elsewhere [17]. The synthetic peptide (referred here as AFQ peptide) with 29 amino-acids long sequence derived from amino-acids 512–540 of FrpC protein (the numbers corresponds to the full-length FrpC protein, Fig. 2a) was produced by Clonestar (purity >96%, MALDI MS, HPLC, Clonestar peptide service).

Titrations of proteins SPM (100 μg/ml, 5 μM) or AFQ (15 μM) with Tb^{3+} by adding small aliquots of $Tb(NO_3)_3$ (typically from 100 μM stock) were performed in Hepes buffer (10 mM HEPES, 50 mM NaCl, pH 7.4). All measurements were performed in a quartz cuvette (volume 50 μl, optical path length 3 mm, Hellma) at 24 °C. The steady state spectra (single photon counting) were recorded using the FluoroMax-3 spectrofluorometer (Horiba Jobin Yvon, France) with the DataMax software (Horiba, Japan). Excitation spectra were recorded in the range of 230–400 nm (bandpass 4 nm) with emission monochromator set to 545 nm (bandpass 7 nm). Long-pass filter 410 nm (3RD410LP, Omega Optical) was inserted into the emission channel to suppress second-order excitation scattering. The resulting spectra were corrected to the background intensity (peptide in buffer). Low intensities of detected phosphorescence can be explained by relatively low concentration of Tb^{3+} used, together with its low molar extinction coefficient and quantum yield. The selectivity of the Tb^{3+} detection was increased by subtracting average background emission intensity at 525 and 565 nm (with practically no Tb^{3+} phosphorescence) from the sharp 545 nm emission peak $IP = (I_{545} - (I_{525} + I_{565}) / 2)$ that corresponds to $^5D_4 \rightarrow {}^7F_5$ transition [18]. This "inner blank" method (Fig. 1) ensures highly specific detection of Tb^{3+} phosphorescence without interference with autofluorescence spectra. The intensity values (IP) presented in Figs. 1, 2 and 3 are counts per second × 10^3.

The tryptophan fluorescence decays I(t), which were used for the lifetime determination, were obtained using FluoroMax-3 equipped with single photon counting controller FluoroHub (Horiba Jobin Yvon) with NanoLED-295 pulse diode (295 nm peak wavelength, <1 ns pulse duration, 1 MHz repetition rate, Horiba Scientific); the Glan-

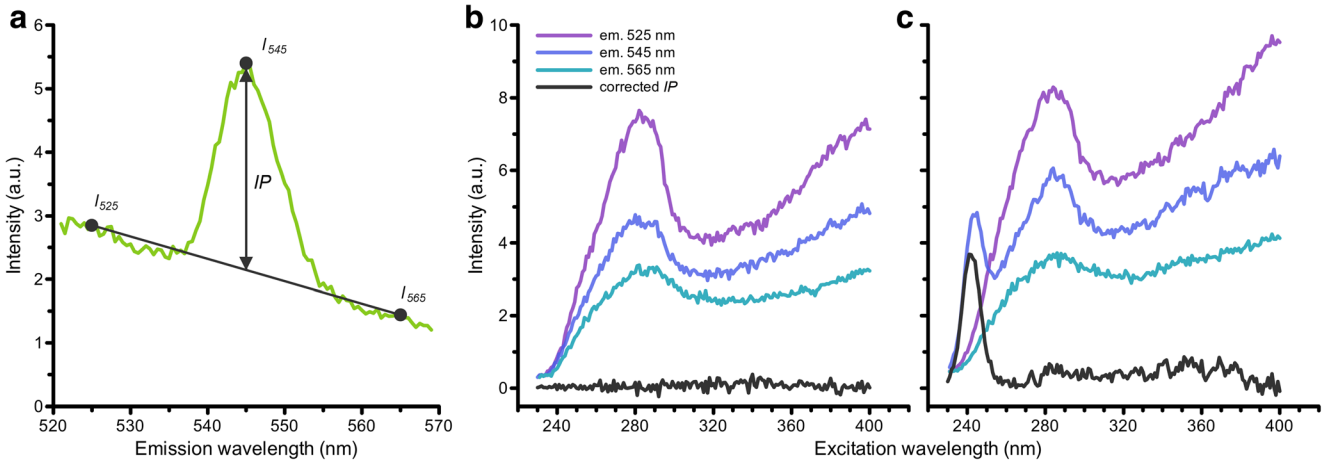

Fig. 1 Detection of low intensities of Tb^{3+} bound to SPM. (**a**) Emission spectrum after 284 nm excitation showing the quantification of phosphorescence intensity. In samples with high level of autofluorescence the intensity of Tb^{3+} phosphorescence (IP, at 545 nm) can be quantified by subtracting the average value of intensities at 525 and 565 nm; $IP = (I_{545} - (I_{525} + I_{565}) / 2)$. (**b**-**c**) Excitation spectra of samples containing (**b**) SPM (5 μM) or (**c**) Tb^{3+} (1 μM) plus SPM (5 μM) recorded at 525, 545 and 565 nm (see legend). Black curves represent the corrected excitation spectra (IP)

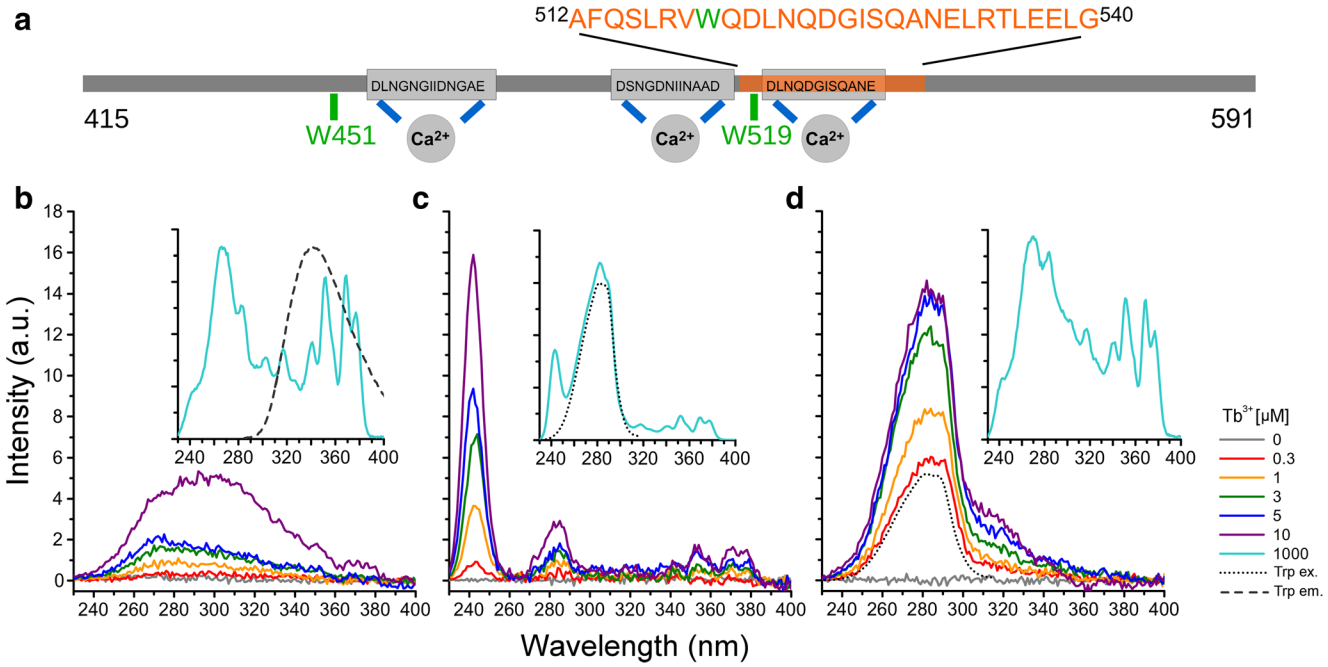

Fig. 2 **a** Amino acid sequence of AFQ peptide and predicted Ca^{2+}-binding sites on SPM protein. The amino acid sequences of putative Ca^{2+}-binding sites (light gray boxes) deduced from sequence homology to canonical EF-hand loop are shown in the SPM protein which comprises residues 415–591 of full-length FrpC protein. The sequence of AFQ peptide (residues 512–540 of FrpC protein) is depicted in orange. The positions of the two Trp residues (Trp451 and Trp519) are highlighted with green. (**b**-**d**) Excitation spectra of terbium at varying Tb^{3+} concentrations (shown right); (**b**) Free Tb^{3+} in HEPES buffer, (**c**) Tb^{3+} with SPM protein. (**d**) Tb^{3+} with AFQ peptide. Insets: the normalized excitation spectra at Tb^{3+} 1000 μM (inset in **b**) in presence of the corresponding peptide (insets in **c** and **d**). The black lines represent the normalized excitation spectrum (**c**, **d** – dotted line, emission at 340 nm) and emission spectrum (**b** – dashed line, excitation at 270 nm) of Trp in AFQ peptide for comparison of spectral overlap

Taylor polarizer was placed at the excitation arm of the fluorometer. The emission monochromator was set to 350 nm with slits of 16 nm while the sheet polarizer was used for the emission path in order to record the emission under "magic-angle" conditions (where intensity does not depend on the rotational diffusion of the fluorophore). Reconvolution analysis of measured fluorescence decays were performed using the DAS6 lifetime fitting software (Horiba Jobin Yvon IBH). Fluorescence intensity in time domain was assumed as three-exponential according to equation:

$$I(t) = A + B_1 \cdot exp(-t/\tau_1) + B_2 \cdot exp(-t/\tau_2) + B_3 \cdot exp(-t/\tau_3) \quad (1)$$

where τ_i are fluorescence lifetimes and B_i are the corresponding amplitudes (fractional contributions), A is a decay shift. The average lifetime of tryptophan (τ_{ave}) was calculated according to equation:

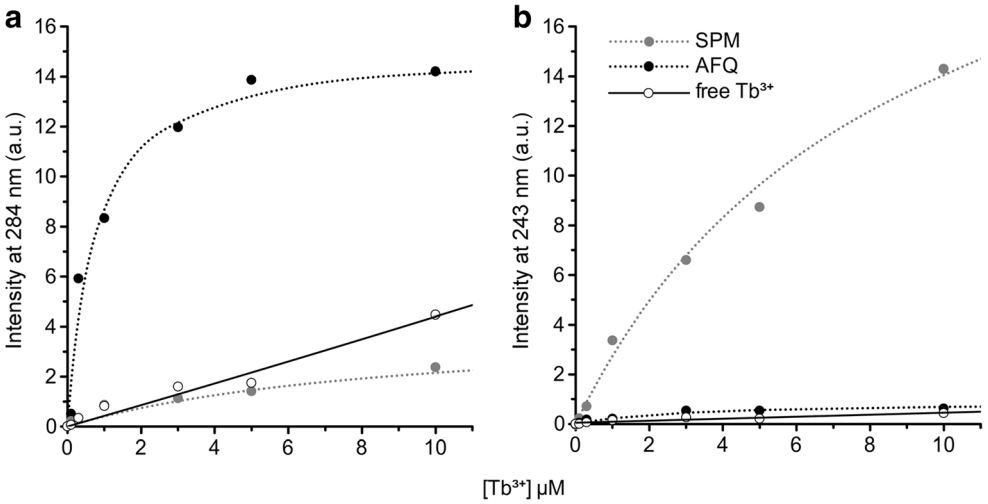

Fig. 3 **Quantification of Trp/Tb^{3+} spectral changes as a function of terbium concentration for the free ions or Tb^{3+} bound to AFQ and SPM (see legend)** Excitation at 284 nm (**a**) and 243 nm (**b**), both emission at 545 nm. The data were fitted by Hill functions (see text for the details)

$$\tau_{ave} = B_1\tau_1 + B_2\tau_2 + B_3\tau_3 \quad (2)$$

where τ_i is particular lifetime and B_i is fractional contribution of each component.

The figures were prepared in Gnumeric 1.12.28 spreadsheet and GIMP 2.8.16 (GNU General Public License).

Results

Spectral Properties of Tb^{3+} – Peptide Complexes

The excitation peaks of terbium can be observed at several wavelengths. In case of free **terbium in buffer** (Fig. 2b), all recorded bands and peaks should represent the fraction of free ions. At lower terbium concentrations (0.3–10 μM) the intensity increases as a broad band (240–360 nm) without resolved distinct peaks. We suppose that the excitation spectrum reflects a non-specific interaction of Tb^{3+} with buffer components [7] used here at relatively high millimolar concentration. At high terbium concentration (1 mM), the distinct excitation peaks are observable (Fig. 2b, inset). By fitting of Gaussian functions to the excitation spectrum, we can distinguish individual peaks from 242 to 377 nm (see Table 1). The excitation spectrum of the free Tb^{3+} ion is dominated by 266 nm maximum.

The Tb^{3+} (0.3–10 μM of added ion) **bound to SPM protein** exerts enhanced excitation at 243 nm and to a lesser extent at 284 nm (Fig. 2c). Both wavelengths represent the direct excitation of the Tb^{3+} ions bound in the multiple binding sites where the water molecules are excluded. At very high Tb^{3+} concentration (1 mM) the excitation at 284 nm prevails (Fig. 2c, inset) suggesting involvement of aromatic residues of the protein in the absorption process (discussed in the next paragraph).

In case of **AFQ peptide** (Fig. 2d), the excitation at 243 nm is missing. Instead, a broad excitation band (250–300 nm) with the peak at 284 nm appears clearly due to the selective enhancement of Tb^{3+} phosphorescence by resonance energy transfer from indolyl group; the terbium ion thus must be bound closely to the tryptophan residue (Trp519) of the peptide. The peak shape corresponds almost exactly to the tryptophan excitation spectrum (Fig. 2d – dotted line, measured at 340 nm tryptophan emission). The excitation peak at 284 nm is predominating until the saturation of binding site of the peptide around 100 μM of Tb^{3+}. At 1 mM Tb^{3+} concentration the excitation spectrum is dominated by the excess of non-bound terbium (Fig. 2d, inset).

The hypothesis of Trp519 → Tb^{3+} energy transfer is supported by the time-resolved fluorescence lifetime data; fluorescence of Trp519 in AFQ peptide (without Tb^{3+}) exerts three-exponential decay curve with average lifetime $<\tau_0>$=3.24 ns. In presence of 1 mM Tb^{3+} ions the Trp519 fluorescence is dynamically quenched showing decreased lifetime $<\tau>$=2.38 ns.

Binding Sites on AFQ Peptide and SPM Protein

The intensity of phosphorescence of **Tb^{3+} in the buffer** depends almost linearly on the Tb^{3+} concentration at any excitation wavelength (Fig. 3, open symbols) as would be expected.

The phosphorescence intensity of Tb^{3+} interacting with the peptide directly describes the fraction of ions bound during the titration. The **Tb^{3+} ions bound to SPM** protein exert the phosphorescence with clear saturation of intensity at higher ion concentration. We plotted the intensity at 284 and 243 nm as a function of added Tb^{3+} (concentration up to 30 μM) and fitted the data with Hill function (Fig. 3, gray symbols). For SPM we obtained apparent dissociation constants K_{D284nm} = 9.14 μM, K_{D243nm} = 8.50 μM and the Hill numbers n_{284nm} = 1.32, n_{243nm} = 1.15 for the 284 and 243 nm excitations, respectively. For both wavelengths we observed the direct Tb^{3+} excitation and most probably we detect the same population of Tb^{3+} ions. In presence of 1 mM Tb^{3+}, the ions probably occupy additional binding sites (Fig. 2c, inset). Nevertheless, at higher Tb^{3+} concentration (>1 mM) we observed SPM protein aggregation which disallowed characterization of the low affinity binding sites.

The titration of **AFQ peptide with Tb^{3+}** ions resulted in dramatic increase of phosphorescence characterized by K_{D284nm} = 0.75 μM and n_{284nm} = 0.83 after 284 nm excitation (Fig. 3a, black symbols). At >5 μM Tb^{3+} the saturation of the binding site was observed and any additional increase of phosphorescence at higher Tb^{3+} concentration could be attributed to the non-bound Tb^{3+}. The direct excitation of AFQ-Tb^{3+} at 243 nm did not produce reproducible results due to the ineffective absorption.

Table 1 Excitation peaks of free Tb^{3+} ions and SPM bound Tb^{3+} at 1 mM concentration (emission at 545 nm)

Sample	Position of excitation peak (nm)									
Free Tb^{3+}	242.4	266.4	283.9	302.8	317.3	326.8	340.9	351.1	368.3	377.0
SPM-Tb^{3+}	243.2	*276.2	*284.1	*291.3	318.2	330.6	340.1	352.7	369.1	377.4

The underlined numbers highlight the dominating peaks. The peaks labeled with * greatly overlap, forming single broad absorption band

Discussion

In this communication we show a very simple way to determine how is the terbium ion bound to protein by recording excitation spectra of terbium phosphorescence. We used the model ion-binding protein with multiple Ca^{2+}-binding sites where the binding of Tb^{3+} was previously described, and the shorter part of this peptide consisting exclusively of one Tb^{3+}-binding site. According to the lifetime data, Trp519 in AFQ peptide has to be in the close contact with bound Tb^{3+} ion; together they form a luminescent complex. Assuming the critical Förster distance $R_0 = 4.10$ [Å] for Trp-Tb^{3+} FRET pair [3], the calculated distance of Trp519 and bound Tb^{3+} ion is 4.85 [Å]. Interestingly, the AFQ-Tb^{3+} complex shows Tb^{3+} phosphorescence with typical tryptophan excitation spectrum which clearly supports the hypothesis of Trp519 → Tb^{3+} energy transfer even at the lowest ion concentrations.

The AFQ binding site is probably freely accessible to water molecules because the direct excitation of Tb^{3+} at 243 nm associated with $4f^8 \rightarrow 4f^7$ 5d electric dipole allowed transitions is undetectable. This suggests the quenching of Tb^{3+} excited state by interaction with high-energy vibrations of O-H bonds [19]. Such interaction with surrounding water molecules were expected since the small AFQ peptide is not able to form hydrophobic pockets due to its short length. In contrast, the Tb^{3+} excitation at 243 nm could be used specifically for quantification of Tb^{3+} bound to dehydrated binding sites on the SPM protein that are absent on the short AFQ peptide.

Interestingly, depending on the shape of the 284 nm excitation peak, this wavelength could be used in some case for direct Tb^{3+} excitation ("narrow peak" of SPM at <10 μM Tb^{3+}) without additional effects of aromatic residues, for specific "FRET excitation" by Trp residue ("broad band" of AFQ peptide) or for the mixed direct and FRET excitation of Tb^{3+} (SPM at 1 mM Tb^{3+}) where multiple binding sites are occupied.

Unfortunately, the apparent dissociation constants of AFQ and SPM in complexes with Tb^{3+} cannot be compared directly because there are five binding sites in SPM protein [17] and we observe only their average properties, whereas AFQ most probably binds single Ca^{2+}/Tb^{3+} ion.

Clearly, the properties of Tb^{3+}-binding site (the sequence WQDLNQDGISQANE) in AFQ peptide and in SPM protein are very different. The residue Trp519 forms a non-fluorescent complex with Tb^{3+} in SPM protein [17]. Therefore, the Trp excitation spectrum that appears at high Tb^{3+} concentrations (Fig. 2b, inset) is most probably caused by Trp451 and not by Trp519 of SPM protein.

The AFQ peptide contains a single aromatic residue. However, we expect that the inevitable absence of Trp451-Trp519 π–π interaction in AFQ peptide allows different Trp519-Tb^{3+} configuration in comparison to that in SPM protein. In AFQ peptide Trp519 retains its proximity to Ca^{2+}-binding site but probably changes its relative orientation. The details of the binding modes should be deciphered e. g. by measurements of circularly polarized luminescence emission spectra [20]. Nevertheless, we show that the engagement of aromatic amino-acid residues in the Tb^{3+}-binding can be studied on the spectral level. In theory, it would be possible to measure the Tb^{3+}-binding at excitation wavelength of 243 nm, to predict the intensity at 284 nm and to compare it with the acquired data at this wavelength. The eventual enhanced excitation should then correspond to additional sensitization of Tb^{3+} emission by FRET process that suggests the involvement of aromatic residues in the binding site.

Conclusion

The sensitivity of the Tb^{3+} detection by steady state phosphorescence is very low, in general. It could be increased by the smart usage of sharp emission peak at 545 nm; the excitation spectrum could be corrected by subtracting the averaged background excitation spectra recorded at both 525 nm and 565 nm emission wavelengths. This should improve the Tb^{3+} detection limits especially in samples with high levels of autofluorescence. Such approach resembles the usage of internal standard in other analytical methods. This new procedure might be important when studying high affinity Tb^{3+}-binding, i. e. using low Tb^{3+} concentrations, by definition.

The study of natural Ca^{2+} binding site using resonance energy transfer from aromatic amino-acid to Tb^{3+} allows to find more detailed structural information. FRET is possible thanks to the overlap of Trp emission (^{1}La transition) and Tb^{3+} excitation spectra at 320–380 nm (representing the transitions from the $^7F_6$ ground state to $^5D_2$, $^5L_9$, $^5L_{10}$, $^5D_3$ levels) (Fig. 2b, inset) with Förster distance about 4 [Å] for Trp-Tb^{3+} pair. The presence of Trp → Tb^{3+} resonance energy transfer could be easily proven by inspecting the whole Tb^{3+} excitation spectrum rather than the mere changes in phosphorescence intensities at selected wavelengths.

The spectral region (around 284 nm) specific for the Tb^{3+} ion bound in proximity to Trp residues is distinct form spectrum of free Tb^{3+} ions (~266 nm or > 320 nm) or of Tb^{3+} ion bound to hydrophobic binding sites (~243 nm). Theoretically, the deconvolution of the spectral components should allow the distinction and characterization of multiple binding sites on single protein molecule. We assume, the proof of Trp → Tb^{3+} energy transfer by observation of the shape of excitation spectra is more robust than quantification of donor quenching (e. g. by lifetime measurement) that could be caused by changes in protein conformation and/or quenching by other amino-acid side chains.

Acknowledgements This work was supported by project SVV 260426 of The Ministry of Education, Youth and Sports and the project 354611 (P.L.) of the Charles University. The authors wish to thank Lucie Jánská

for excellent technical assistance and Dr. Zdeněk Fišar for borrowing the pulse diode.

Compliance with Ethical Standards

Conflict of Interest The authors declare that they have no conflict of interest.

References

1. Schlyer BD, Steel DG, Gafni A (Sep. 1995) Direct kinetic evidence for triplet state energy transfer from *Escherichia coli* alkaline phosphatase tryptophan 109 to bound terbium. J Biol Chem 270(39): 22890–22894
2. Basu G, Allen M, Willits D, Young M, Douglas T (Sep. 2003) Metal binding to cowpea chlorotic mottle virus using terbium(III) fluorescence. J Biol Inorg Chem 8(7):721–725
3. Canada RG, Paltoo DN (Nov. 1998) Binding of terbium and cisplatin to C13* human ovarian cancer cells using time-resolved terbium luminescence. Biochim Biophys Acta-Mol Cell Res 1448(1): 85–98
4. Horrocks WD (1982) Lanthanide ion probes of biomolecular structure. Adv Inorg Biochem 4:201–261
5. Brittain HG, Richardson FS, Martin RB (1976) Terbium(III) emission as a probe of calcium(II) binding sites in proteins. J Am Chem Soc 98(25):8255–8260
6. Lakowicz JR (2006) Principles of fluorescence spectroscopy, 3rd edn. Springer US, Boston, pp XXVI, 954. https://doi.org/10.1007/978-0-387-46312-4
7. Miller TL, Bennet LW, Spatz DS (1986) Terbium luminescence from complexes of angiotensin II, small peptides, and amino acids. Ohio J Sci 86(4):140–143
8. Jiao M et al (2013) Synthesis, structure and photoluminescence properties of europium-, terbium-, and thulium-doped Ca3Bi(PO4)3 phosphors. Dalton Trans 42(34):12395–12402
9. Guo L, Yan B, Liu J-L, Sheng K, Wang X-L (2011) Coordination bonding construction, characterization and photoluminescence of ternary lanthanide (Eu^{3+}, Tb^{3+}) hybrids with phenylphenacylsulfoxide modified bridge and polymer units. Dalton Trans 40(3): 632–638
10. Tran TH, Tran KA, Hoang TK, Pham TH, Le QM (2012) Fabrication and properties of terbium phosphate nanorods. Adv Nat Sci Nanosci Nanotechnol 3(1):015010
11. Ladokhin AS (2000) Fluorescence spectroscopy in peptide and protein analysis. In: Schoneich C (ed) Peptides and proteins (Encyclopedia of analytical chemistry: applications of instrumental methods). Wiley, New York. https://doi.org/10.1002/9780470027318.a1611
12. Ohara P (1987) Lanthanide ions as luminescent probes of biomolecular structure. Photochem Photobiol 46(6):1067–1070
13. DeJersey J, Morley P, Martin R (1981) Lanthanide probes in biological-systems - characterization of luminescence excitation-spectra of terbium complexes with proteins. Biophys Chem 13(3): 233–243
14. Dieke GH (Mar. 1970) Spectra and energy levels of rare earth ions in crystals. Am J Phys 38(3):399–400
15. de Graaf D, Stelwagen SJ, Hintzen HT, de With G (Sep. 2003) Tb^{3+} luminescence as a tool to study clustering of lanthanide ions in oxynitride glasses. J Non-Cryst Solids 325(1):29–33
16. Osicka R, Prochazkova K, Sulc M, Linhartova I, Havlicek V, Sebo P (Jun. 2004) A novel 'clip-and-link' activity of repeat in toxin (RTX) proteins from gram-negative pathogens - covalent protein cross-linking by an asp-Lys isopeptide bond upon calcium-dependent processing at an asp-pro bond. J Biol Chem 279(24): 24944–24956
17. Liskova PM et al (2016) Probing the Ca^{2+}-assisted π-π interaction during Ca^{2+}-dependent protein folding. Soft Matter 12(2):531–541
18. Bala M et al (2018) Synthesis, photoluminescence behavior of green light emitting Tb(III) complexes and mechanistic investigation of energy transfer process. J Fluoresc 28(3):775–784
19. Caldiño U, Speghini A, Bettinelli M (2006) Optical spectroscopy of zinc metaphosphate glasses activated by Ce^{3+} and Tb^{3+} ions. J Phys Condens Matter 18(13):3499–3508
20. Neil ER, Fox MA, Pal R, Pålsson L-O, O'Sullivan BA, Parker D (2015) Chiral probe development for circularly polarised luminescence: comparative study of structural factors determining the degree of induced CPL with four heptacoordinate europium(III) complexes. Dalton Trans 44(33):14937–14951